

BASIC COMPRESSIBLE FLOW OVER A ROTATING DISK

M. Türkyilmazoğlu* and N. Uygun*

Received 02:01:2003 : Accepted 09:08:2004

Abstract

In this work the basic flow field is investigated for the compressible boundary layer flow over a rotating disk. Making use of self-consistent assumptions within boundary layer theory, the governing basic equations of motion are derived leading to a generalized steady compressible Von Karman flow. A Runge-Kutta integration method accurate to the fourth order is then employed for the solution of the resulting equations. Finally the velocity and temperature distributions corresponding to the various parameters are calculated numerically and presented.

Keywords: Compressible flow, Rotating-disk boundary layer, Runge-Kutta integrator.

2000 AMS Classification: 46F10

1. Introduction

The boundary layer flow due to a rotating disk has received substantial interest, in particular during the last two decades, since it constitutes a prototype for the flow over modern aircraft wings. Its significance lies in the fact that owing to the resemblance of the mean velocity profiles in cross flow directions, most of the fluid dynamical properties of the flow over a rotating disk and a swept-back wing almost coincide as far as the nature of instabilities is concerned. To be more precise, both flows are subject to cross flow vortices leading to convective or absolute instabilities.

A series of studies have been conducted to understand the reasons behind the instability mechanisms in three-dimensional boundary layer flows. Among these, the theoretical works of Gregory, Stuart and Walker [7], Malik [15], Malik, Wilkinson and Orszag [17], Mack [14], Hall [8], Bassom and Gajjar [3], Balakumar and Malik [2], Lingwood [11] and Turkyilmazoglu [21] have highlighted the inevitable instabilities caused by the stationary or, in some circumstances, travelling disturbances. In particular, the latest two works have demonstrated that unlike the convective instability mechanism which arises in most three-dimensional boundary layer flows, the rotating disk boundary layer flow is subjected to absolute instability. Although the earlier experiments by Gregory, Stuart

*Mathematics Department, University of Hacettepe, 06532-Beytepe, Ankara, Turkey.
E-mail : turkyilm@hotmail.com

and Walker [7], Wilkinson and Malik [23], and Kohama [10] were only able to detect convective type instability, the more recent experiment carried out by Lingwood [12] has given an apparent support for the existence of absolute instability over a rotating disk.

The aforementioned stability studies require genuine basic velocity profiles, which, for the incompressible flow case, is the well known Von Karman's basic steady flow. On the other hand, the compressible basic flow is much more complicated to evaluate. This is because, as pointed out by Stewartson [20] and others, there are several parameters involved in the compressible flow case, such as the Prandtl number and the second coefficient of viscosity which are not even constants as they are in the incompressible case. Our motivation here is, therefore, to devise an approach which will involve a series of approximation to obtain the basic compressible equations for the three dimensional rotating disk boundary layer flow that we will call the generalized Von Karman's flow. The ultimate goal of the research is to investigate the character of the instabilities existing in this generalized Von Karman's flow, which is currently under investigation and will be reported elsewhere.

The present study is organized in the following manner. The governing equations of motion and the derivation of the mean flow equations are presented in section 2. Next, the numerical scheme and the results corresponding to several parameters are given in section 3. Conclusions are finally drawn in section 4.

2. Derivation of the Mean Flow Equations

Here, we deal with the compressible three-dimensional boundary layer flow over a rigid disk rotating about its axis with a constant angular velocity Ω in the cylindrical coordinates (r, θ, z) , having been made dimensionless with respect to a reference length scale l which can be taken to be the local radius of the disk. Velocities are non-dimensionalized by $l\Omega$, while the pressure is by $l^2\Omega^2$. Moreover, the density and the temperature of the fluid are non-dimensionalized with respect to their free-stream values. As a consequence, the corresponding unsteady Navier-Stokes equations governing the motion can be expressed in the form

$$(2.1) \quad \frac{\partial \rho}{\partial t} + \nabla \cdot (\rho \mathbf{u}) = 0,$$

$$(2.2) \quad \rho \left[\frac{\partial \mathbf{u}}{\partial t} + (\mathbf{u} \cdot \nabla) \mathbf{u} + 2(\hat{k} \times \mathbf{u}) - r\hat{r} \right] = -\nabla p + \frac{1}{Re} [\nabla(\lambda \nabla \cdot \mathbf{u}) + \nabla(\mu e_{ij})],$$

$$(2.3) \quad \gamma M_\infty^2 p = \rho T,$$

$$(2.4) \quad \rho \left[\frac{\partial T}{\partial t} + (\mathbf{u} \cdot \nabla) T \right] = M_\infty^2 (\gamma - 1) \left[\frac{\partial p}{\partial t} + (\mathbf{u} \cdot \nabla) p \right] + \frac{1}{Re} [\nabla \cdot (k \nabla T) + \frac{\gamma - 1}{Re} M_\infty^2 [\frac{1}{2} \mu (e_{11}^2 + e_{22}^2 + e_{33}^2 + 2e_{12}^2 + 2e_{13}^2 + 2e_{23}^2) + \lambda (\nabla \cdot \mathbf{u})^2]].$$

It should be remarked that the viscous, Coriolis and streamline curvature effects are all included in equations (2.1-2.4). Equation (2.1) is the continuity equation, equation (2.2) is the momentum equation in vector form, Equation (2.3) is the equation of state and Equation (2.4) the energy equation, respectively. Together with these equations, the appropriate boundary conditions are the usual no-slip condition on the wall except the azimuthal velocity in the θ direction (though, the extra r term appearing in equation (2.2) allows the azimuthal velocity to disappear on the wall as well), and the vanishing quantities at the far-field apart from the uniform temperature. The several parameters appearing in equations (2.1-2.4) are defined as follows; ρ the density, \mathbf{u} the velocity

vector, ∇ the usual gradient operator in cylindrical coordinates, p the pressure, T the temperature. Moreover, the strain tensors are defined by

$$\begin{aligned} e_{11} &= 2\frac{\partial u}{\partial r}, & e_{12} = e_{21} &= r\frac{\partial}{\partial r}\left(\frac{v}{r}\right) + \frac{1}{r}\frac{\partial u}{\partial \theta}, & e_{13} = e_{31} &= \frac{\partial u}{\partial z} + \frac{\partial w}{\partial r}, \\ e_{22} &= 2\left(\frac{1}{r}\frac{\partial v}{\partial \theta} + \frac{u}{r}\right), & e_{23} = e_{32} &= \frac{1}{r}\frac{\partial w}{\partial \theta} + \frac{\partial v}{\partial z}, & e_{33} &= 2\frac{\partial w}{\partial z}. \end{aligned}$$

Furthermore, μ is the dynamical viscosity, λ the second coefficient of viscosity related to the bulk viscosity, γ the ratio of the specific heats, M_∞ the free stream Mach number, Re the Reynolds number characterizing the flow defined by $Re = \frac{\Omega l^2}{\nu}$, and finally k is the parameter associated with the Prandtl number σ . The Reynolds number is taken to be large in the following analysis.

The basic flow of the incompressible case, also called the Von Karman's steady state flow, is well known since the work of Kármán [9]. The steady compressible flow, hereafter to be termed the generalized Von Karman's flow, will be considered here using a series of approximations in line with the boundary layer flow assumption. First of all, the basic flow is assumed to evolve alongside the boundary layer coordinate $\xi = Re^{1/2}z$, which is of order unity. The flow being axisymmetric about the axis of rotation entails all derivatives with respect to θ to vanish. Taking these into account, if we substitute the basic flow velocities ($u_B, v_B, Re^{-1/2}w_B$) and the other quantities into the governing equations (2.1-2.4), and also neglect terms of $O(Re^{-1})$, the mean flow quantities are determined from the subsequent equations and boundary conditions:

$$(2.5) \quad \rho_B\left(\frac{\partial u_B}{\partial r} + \frac{\partial w_B}{\partial \xi}\right) + u_B\frac{\partial \rho_B}{\partial r} + w_B\frac{\partial \rho_B}{\partial \xi} + \frac{\rho_B u_B}{r} = 0,$$

$$(2.6) \quad \rho_B\left(u_B\frac{\partial u_B}{\partial r} + w_B\frac{\partial u_B}{\partial \xi} - \frac{v_B^2}{r} - 2v_B - r\right) = -\frac{\partial p_B}{\partial r} + \frac{\partial}{\partial \xi}\left(\mu_B\frac{\partial u_B}{\partial \xi}\right),$$

$$(2.7) \quad \rho_B\left(u_B\frac{\partial v_B}{\partial r} + w_B\frac{\partial v_B}{\partial \xi} + \frac{u_B v_B}{r} + 2u_B\right) = \frac{\partial}{\partial \xi}\left(\mu_B\frac{\partial v_B}{\partial \xi}\right),$$

$$(2.8) \quad \frac{\partial p_B}{\partial \xi} = 0,$$

$$(2.9) \quad \gamma M_\infty^2 p_B = \rho_B T_B,$$

$$(2.10) \quad \rho_B\left(u_B\frac{\partial T_B}{\partial r} + w_B\frac{\partial T_B}{\partial \xi}\right) = M_\infty^2(\gamma - 1)\left\{u_B\frac{\partial p_B}{\partial r} + w_B\frac{\partial p_B}{\partial \xi} + \mu_B\left[\left(\frac{\partial u_B}{\partial \xi}\right)^2 + \left(\frac{\partial v_B}{\partial \xi}\right)^2\right]\right\} + \frac{\partial}{\partial \xi}\left(k_B\frac{\partial T_B}{\partial \xi}\right),$$

$$u_B = v_B = w_B = 0 \text{ at } \xi = 0,$$

$$(2.11) \quad u_B \rightarrow 0, \quad v_B \rightarrow -r \text{ as } \xi \rightarrow \infty,$$

$$\rho_B, T_B, \mu_B \rightarrow 1, \quad p_B \rightarrow \frac{1}{\gamma M_\infty^2} \text{ as } \xi \rightarrow \infty.$$

In contrast to the case of incompressible flow, it should be noticed that since we consider the fluid to be a perfect gas in the state equation (2.9), and further, since the fluid is stationary everywhere outside the boundary layer, it is straightforward to deduce from equations (2.8-2.9) and (2.11) that p_B is constant and equal to $(\gamma M_\infty^2)^{-1}$. Secondly, we will assume the Chapman's viscosity law, that is, $\mu = CT$ for some constant C . Such an approximation is particularly shown to be useful for low Mach numbers, see for instance Stewartson [20] and Papageorgiou [18]. Furthermore, despite the fact that the bulk viscosity does not enter into the following analysis, having been cancelled out by the large Reynolds number limit, experimental researches prove that viscosity coefficients can be taken as a function of temperature only, and for a monatomic gas $\lambda = -\frac{2}{3}\mu$ is

generally a good choice, see for instance Rosenhead [19]. Thirdly, to remove the density terms from the mean flow equations (2.5-2.11), we make use of the Doronitsyn-Howarth transformation, that is, $y = C^{-1/2} \int_0^\xi \rho_B d\xi$ as given in Stewartson [20]. In the light of the previous assumptions and taking into consideration the strategies of the incompressible Von Karman's flow, the form of the generalized Von Karman's flow may be written as

$$u_B = (u_B, v_B, w_B, p_B) = (r\bar{u}(y), r\bar{v}(y), \bar{w}(y), \frac{1}{\gamma M_\infty^2}).$$

Eventually, making use of the stream function formulae automatically satisfying Equation (2.5), that is,

$$\bar{u} = \frac{d\psi}{dy} = \psi'(y), \quad \bar{w} = -C^{1/2} T_B (2\psi + r\psi' \frac{\partial y}{\partial r}),$$

will greatly simplify the form of Equations (2.5-2.11).

Keeping in mind all the above assumptions and doing the necessary substitutions into equations (2.5-2.11), the subsequent equations and boundary conditions will result in respectively

$$(2.12) \quad \psi''' = \psi'^2 - 2\psi\psi'' - (\bar{v} + 1)^2,$$

$$(2.13) \quad \bar{v}'' = 2(\bar{v} + 1)\psi' - 2\psi\bar{v}',$$

$$(2.14) \quad \frac{\partial^2 T_B}{\partial y^2} + 2\sigma\psi \frac{\partial T_B}{\partial y} - r\sigma\psi' \frac{\partial T_B}{\partial r} + (\gamma - 1)\sigma r^2 M_\infty^2 (\psi''^2 + \bar{v}'^2) = 0,$$

$$(2.15) \quad \psi(0) = \psi'(0) = \psi(\infty) = \bar{v}(0) = \bar{v}(\infty) + 1 = T_B(\infty) - 1 = 0.$$

The system (2.12-2.15) is called the generalized Von Karman's equations for the compressible flow for short. Although the Karman equations (2.12-2.13) are well known to exhibit infinite degrees of non-uniqueness, the solution that we have obtained in the coming section under the constraints (2.15) are physically expected ones because they absolutely match with the experimentally determined profiles, see for instance Lingwood [13], which have been used for several instability investigations, amongst these being Malik [15], Hall [8] and Balakumar and Malik [2]. In addition to this, it can be easily seen that the influence of the compressibility comes into effect owing to the temperature field given in (2.14), which significantly alters the flow field from the incompressible case. Now supposing that the temperature field in (2.14) can be written in terms of a viscous dissipation term f and a heat conducting term q , it is possible to express it in the form

$$(2.16) \quad T_B = \frac{1}{\rho_B} = 1 - \frac{\gamma - 1}{2} M_r^2 f(y) + (T_w - 1)q(y),$$

which allows the splitting of the energy equation into two ordinary differential equations

$$(2.17) \quad \begin{aligned} f'' + 2\sigma\psi f' - 2\sigma\psi' f &= 2\sigma(\psi''^2 + \bar{v}'^2), \\ q'' + 2\sigma\psi q' &= 0. \end{aligned}$$

The parameter M_r appearing in equation (2.16) is the local Mach number defined by $M_r = rM_\infty$. Moreover, taking into account the far-field uniform temperature in (2.11), $f = q = 0$ as $y \rightarrow \infty$. However, for an insulated disk, $\frac{\partial T}{\partial y}(0) = 0$ requiring $f'(0) = q'(0) = 0$, leading to $q \equiv 0$. Taking into consideration the heat transfer on the wall, that is $T(0) = T_w$, we have $f(0) = q(0) - 1 = 0$. Additionally, the heat conducting term q in (2.17) can be solved analytically as $q = \int_y^\infty e^{-2\sigma \int_0^y \psi dy} dy / \int_0^\infty e^{-2\sigma \int_0^y \psi dy} dy$ for any prescribed σ , whereas the function f cannot be solved analytically from equation (2.17), therefore, it needs to be treated numerically apart from the perfect fluid case $\sigma = 1$, for which the insulated disk results in $f = \psi'^2 + \bar{v}^2 - 1$ and heat transfer gives rise to $f = \psi'^2 + \bar{v} + \bar{v}^2$.

A further thing worthy of mentioning is the boundary layer thickness. Having obtained the temperature distributions from (2.16), the physically dimensionless quantity z can be recovered as

$$(2.18) \quad z = C^{1/2} Re^{-1/2} \int_0^y T_B dy = C^{1/2} Re^{-1/2} \left\{ y - \frac{\gamma-1}{2} M_r^2 \int_0^y f dy + (T_w - 1) \int_0^y q dy \right\}.$$

Equation (2.18) clearly indicates the stretching effect of the compressibility. It can also be deduced from (2.18) that the distance from the disk surface at which the same value of the azimuthal velocity is attained differ for compressible and incompressible fluids not only by a term proportional to M_r^2 , which in turn depends on the radial distance, but also by the wall temperature values.

3. Numerical Scheme, Results and Discussions

In this section, the numerical procedure used to solve equations (2.12-2.17) will be briefly presented first, followed by the numerical results. A fourth-order accurate Runge-Kutta scheme is employed in conjunction with a shooting technique to match the variables at infinity. Such a technique has been successfully applied to many boundary layer flow problems, for example see Cebeci [6] and Canuto, Hussaini, Quarteroni and Zang [5]; and to hydrodynamic stability calculations, see for example Arnal [1] and Turkyilmazoglu, Gajjar and Ruban [22]. The incompressible steady boundary layer flow over a rotating disk was obtained in Lingwood [12, 13] by means of this method and in Turkyilmazoglu [21] using a Spectral Chebyshev collocation scheme. Based on our experience, the Runge-Kutta method is more straightforward to implement than other methods. To check out the accuracy of the numerical scheme, as well as to validate the code, we first solved as a test case the well known Blasius boundary layer flow over a flat plate, which is governed by the differential equation

$$f''' + \frac{1}{2} f f'' = 0, \quad f(0) = f'(0) = f'(\infty) - 1 = 0.$$

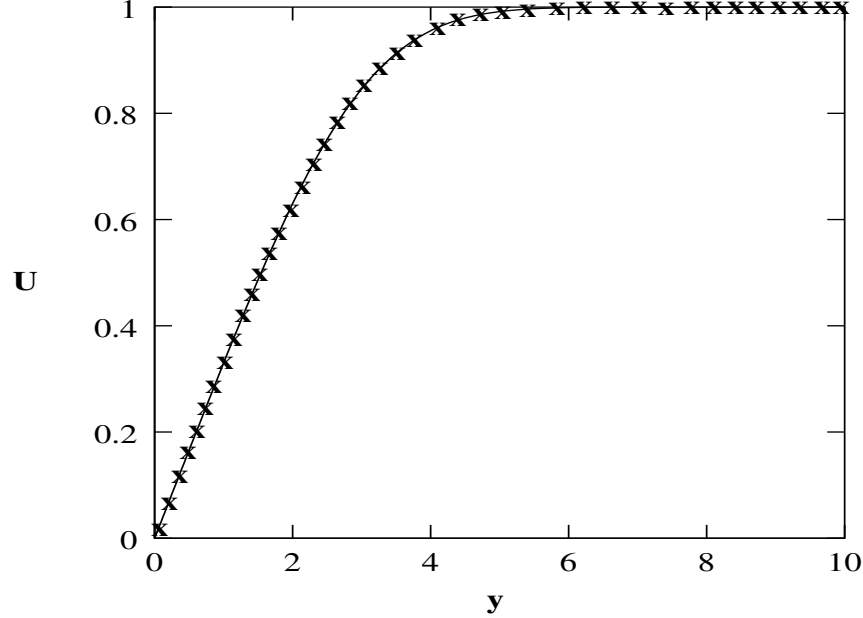
A comparison with the result of Brown [4] is demonstrated in figure 1, which is clear evidence of the accuracy of the numerical method.

Next, with the algorithm at hand, several test cases are considered so that the unknown initial conditions and the far field would not influence the outcomes within the accuracy of the method and machine precision. To be more specific, the domain of integration was fixed to 20 and divided into a 10000 uniform grid, and the integration was performed to give the initial values of $\psi''(0) = 0.51023$, $\bar{v}'(0) = -0.61592$, which are in excellent agreement with the values given in Malik [15].

Further properties of the basic velocity field can be captured from the graph shown in Figure 2(a). These profiles are in fact the same profiles as the Von-Karman's basic incompressible flow over a rotating disk and have been verified to be true in several studies, such as Lingwood [12, 13] and Malik [15], amongst others (see Figure 1 of Lingwood [11], Figure 4 of Lingwood [12] and Figure 2 of Balakumar and Malik [2]). In spite of the fact that these profiles are not the exact compressible flow profiles since they were obtained as a result of a series of self-consistent approximations, nevertheless we will use them for stability investigations of the generalized compressible Von-Karman's boundary layer flow.

Figure 1.

The Blasius profile $U = f'$ is shown against the normal coordinate y . A comparison of the solution obtained from the fourth order Runge-Kutta scheme employed for the present research is displayed with the solution of Brown [4] shown by the crosses.



Equations (2.16–2.17) were then solved to compute the various temperature profiles corresponding to the several Mach numbers, Prandtl numbers and the wall temperatures as depicted in Figures (2–4). The insulated wall case is demonstrated first in Figures 2(b–d) for three different Prandtl numbers and with varying Mach numbers. The overall shapes of the profiles are seen to be similar and the influence of the Prandtl number is to change slightly the wall temperature.

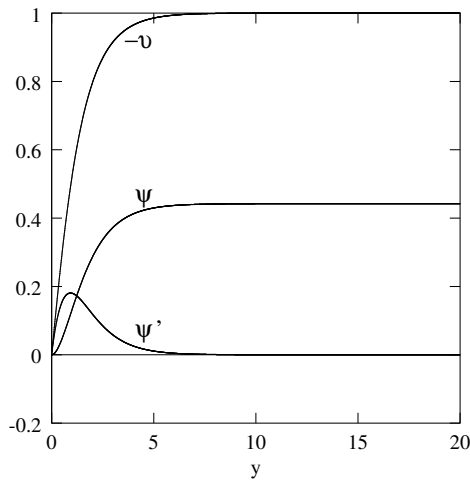
The effect of the heat transfer and Prandtl number can be visualized next in Figures (3–4). It can be inferred from these pictures that the wall heating/cooling has a big impact on the formation of the temperature profiles. Although the far-field behavior of the profiles may be pursued using asymptotic means, it has not been implemented here. It is these graphs in Figures (2–3) that will determine the nature of the instabilities existing in the compressible generalized Von-Karman's flow. As mentioned above, this issue is currently under investigation.

4. Conclusions

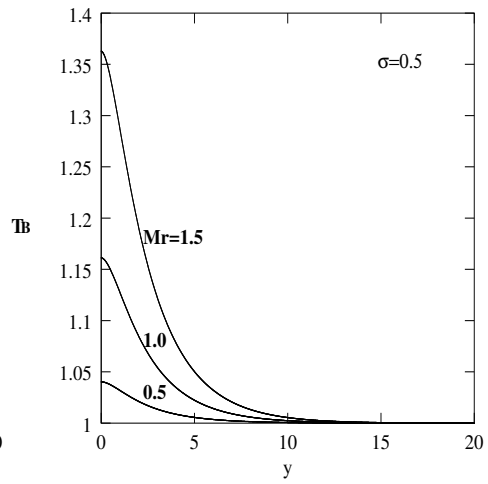
The basic velocity field governing the compressible boundary layer flow over a rotating disk has been obtained using self-consistent assumptions. The resulting equations have then been solved numerically by a Runge-Kutta integrator accurate to the fourth order, and the behavior of the basic velocity and temperature field displayed graphically. The profiles determined will ultimately serve to explore the character of the compressible flow and this will constitute the basis of the oncoming research.

Figure 2.

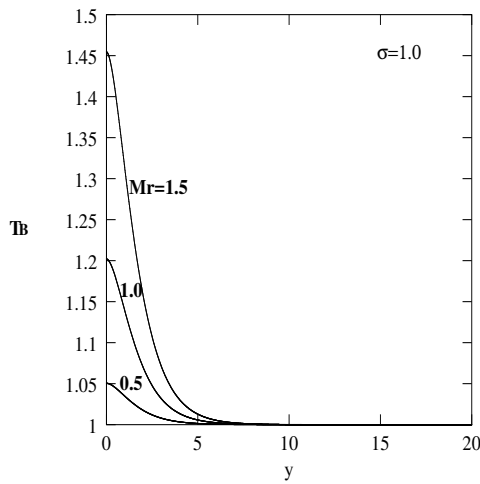
(a) Basic velocity profiles of the generalized Von Karman's flow are shown for the boundary layer over the rotating disk. Temperature profiles for an insulated disk are shown in (b) for $\sigma = 0.5$, in (c) for $\sigma = 1$ and in (d) for $\sigma = 1.5$.



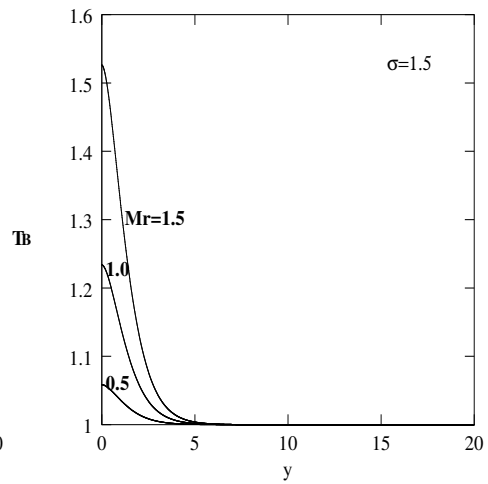
(a)



(b)



(c)



(d)

Figure 3.

Temperature profiles corresponding to the heat transfer case are shown at three different local Mach numbers, respectively in (a) for $\sigma = 0.5$, $T_w = 0.5$, in (b) for $\sigma = 0.5$, $T_w = 1.5$, in (c) for $\sigma = 1.0$, $T_w = 0.5$ and in (d) for $\sigma = 1.0$, $T_w = 1.5$. Dotted curves denote $M_r = 0.0$, straight curves $M_r = 0.5$ and broken curves $M_r = 1.5$.

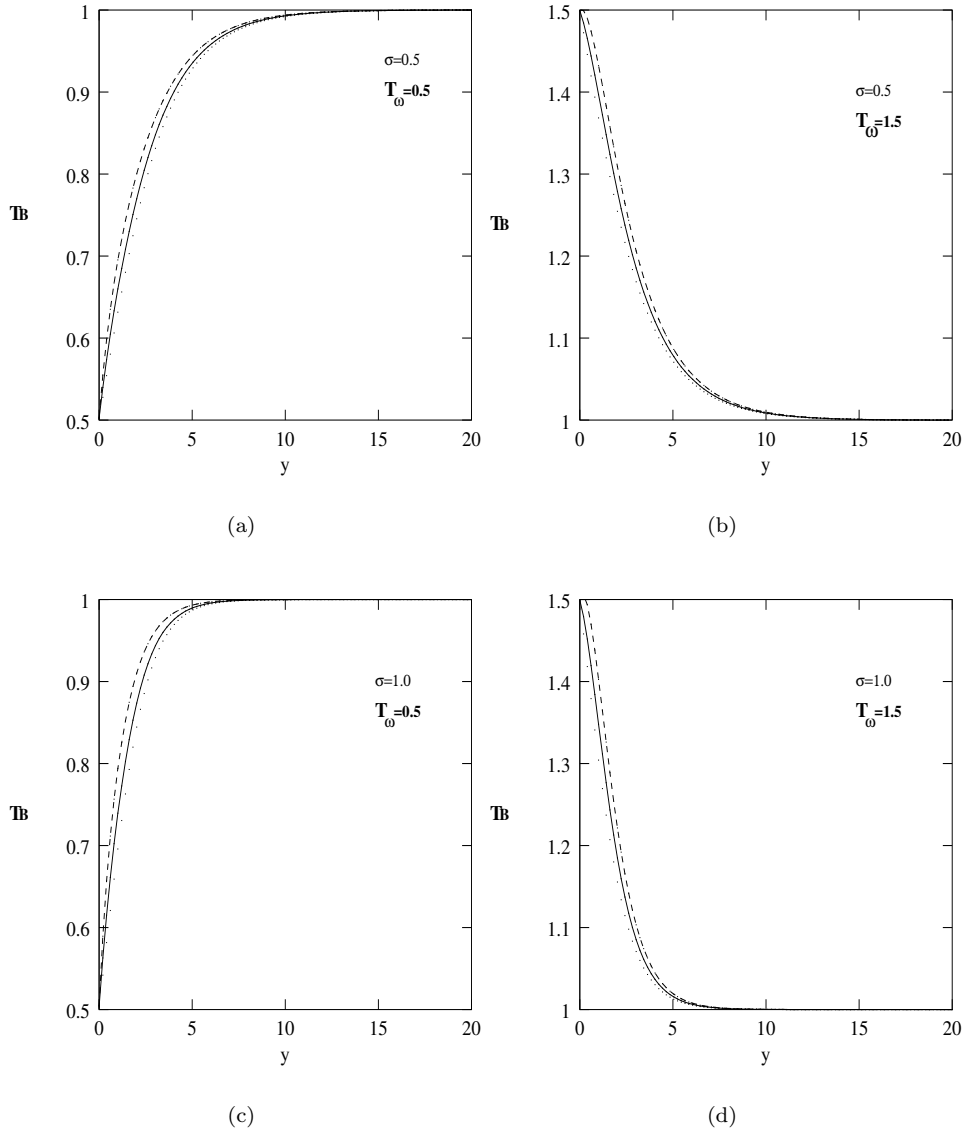
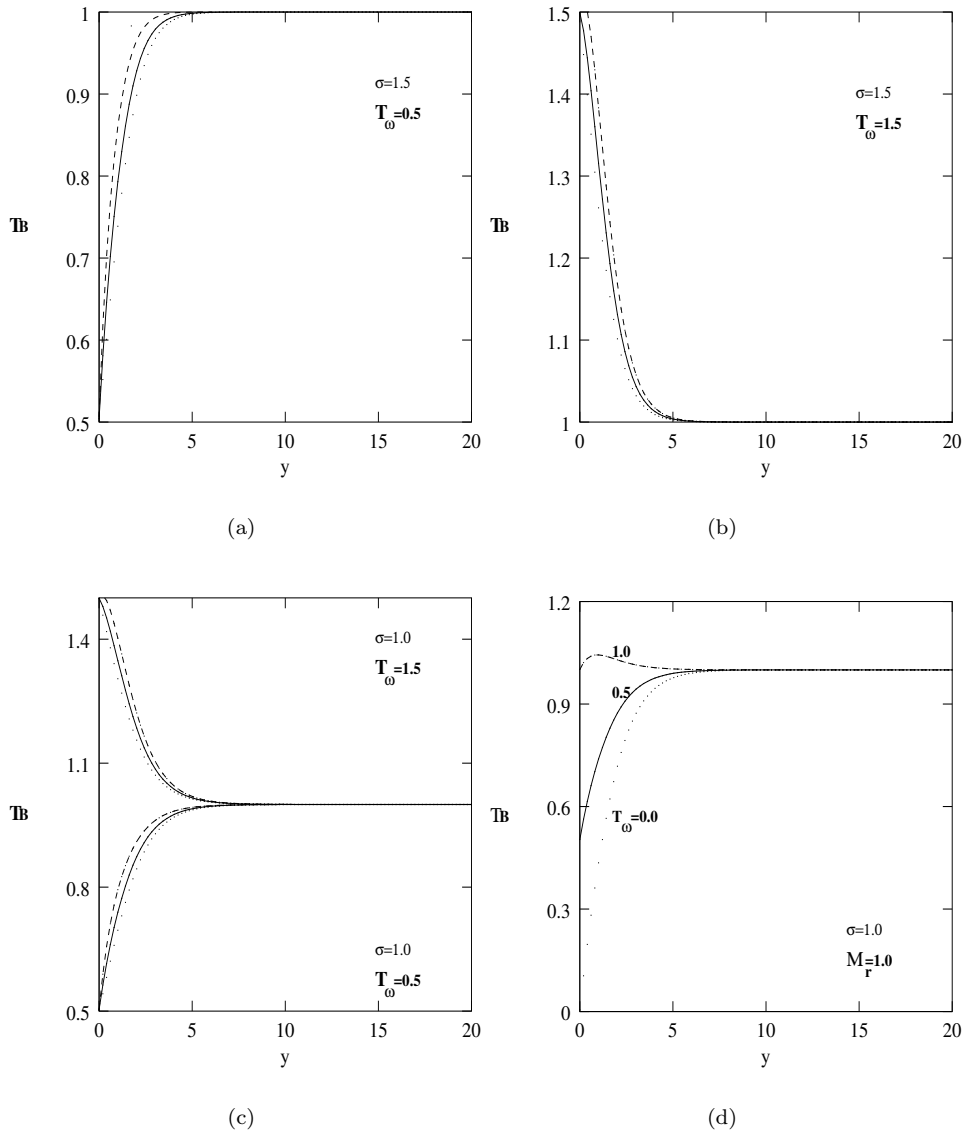


Figure 4

Temperature profiles corresponding to the heat transfer case are shown at three different local Mach numbers respectively, in (a) for $\sigma = 1.5$, $T_w = 0.5$ and in (b) for $\sigma = 1.5$, $T_w = 1.5$. Figures 3(c–d) are redisplayed in combined form in (c). The effect of wall cooling is demonstrated in (d) for $\sigma = 1.0$, $M_r = 1.0$.



References

- [1] Arnal, D. *Boundary layer transition: predictions based on linear theory*, (AGARD-VKI Special Course on Progress in Transition Modelling, 1993).
- [2] Balakumar, P. and Malik, M. R. *Travelling disturbances in rotating-disk flow*. Theoret. Comput. Fluid Dyn. **2**, 125–137, 1990.
- [3] Bassom, A. P. and Gajjar J. S. B. *Non-Stationary cross-flow vortices in a three-dimensional boundary-layer*. Proc. Roy. Soc. London Ser. A **417**, 179–212, 1988.
- [4] Brown, W. B. *Numerical calculation of the stability of cross flow profiles in laminar boundary layers on a rotating-disk and on a swept-wing and an exact calculation of the Blasius velocity profile*. (Northrop Aircraft Inc. Hawthorne, L. A. 59. 1959).
- [5] Canuto, C., Hussaini, M. Y., Quarteroni, A. and Zang, T. A. *Spectral methods in fluid dynamics*, (Springer-Verlag, 1988).
- [6] Cebeci, T. *Numerical and physical aspects of aerodynamic flows*. (Springer-Verlag, 1981–1983–1985).
- [7] Gregory, N., Stuart, J. T. and Walker, W. S. *On the stability of three-dimensional boundary-layers with applications to the flow due to a rotating-disk*. Philos. Trans. R. Soc. London Ser. A **248**, 155–199, 1955.
- [8] Hall, P. *An investigation of the stationary modes of instability of the boundary layer on a rotating-disk*. Proc. Roy. Soc. London Ser. A **406**, 93–106, 1986.
- [9] Kármán, T. V. *Über laminare und turbulente Reibung*. Zeitschnift für angewandte Mathematik und Mechanik. **1**, 233–252, 1921.
- [10] Kohama, Y. *Study on boundary-layer transition of a rotating-disk*. Acta Mech. **50**, 193–199, 1984.
- [11] Lingwood, R. J. *Absolute instability of the boundary layer on a rotating-disk*. J. Fluid Mech. **299**, 17–33, 1995.
- [12] Lingwood, R. J. *An experimental study of absolute instability of the rotating-disk boundary-layer flow*. J. Fluid Mech. **314**, 373–405, 1996.
- [13] Lingwood, R. J. *On the application of the Briggs’ and steepest-descent method to a boundary layer flow*. Stud. Appl. Math. **98**, 213–254, 1997.
- [14] Mack, L. M. *The wave pattern produced by a point source on a rotating-disk*. (AIAA Pap. No. 0490. 1985).
- [15] Malik, M. R. *The neutral curve for stationary disturbances in rotating-disk flow*. J. Fluid Mech. **164**, 275–287, 1986.
- [16] Malik, M. R. and Poll, D. I. A. *Effect of curvature on three-dimensional boundary-layer stability*. AIAA Journal **23**, 1362–1369, 1985.
- [17] Malik, M. R., Wilkinson, S. P. and Orszag, S. A. *Instability and transition in rotating-disk flow*. AIAA Journal **19**, 1131–1138, 1981.
- [18] Papageorgiou, D. T. *The stability of two dimensional wakes and shear layers at high Mach numbers*. Phys. Fluids **3**, 793–802, 1991.
- [19] Rosenhead, L. *Laminar boundary layers*. (Oxford University Press, 1963).
- [20] Stewartson, K. *The theory of laminar boundary layers in compressible fluids*, (Oxford University Press, 1964).
- [21] Türkyılmazoğlu, M. *Linear Stability analysis of two and three-dimensional flows*, (PhD thesis, University of Manchester, 1998).
- [22] Türkyılmazoğlu, M., Gajjar, J. S. B. and Ruban, A. I. *The absolute instability of thin wakes in an incompressible/compressible fluid*, Theoret. Comput. Fluid Dyn. **13**, 91–114, 1999.
- [23] Wilkinson, S. P. and Malik, M. R. *Stability experiments in rotating-disk flow*. (AIAA Pap. No. 1760, 1983).